

# Preparation of RBPM-Ru based on FPSu and its characterization through image segmentation

Kothandaraman D\*<sup>1</sup> and Krishnaveni V<sup>2</sup>

<sup>1</sup>School of Computer Science and Artificial Intelligence, SR University, Warangal, Telangana - 506371, India

<sup>2</sup>Department of Chemistry, Anna University, Chennai 600025, Tamil Nadu, India

(Received October 30, 2020, Revised April 7, 2021, Accepted October 18, 2021)

**Abstract.** A membrane technology is one of the basic categories of water purification technologies that are used to treat wide range of salinity water from brackish to sea water. Bipolar membrane (BPM) is a special type of catalytic ion exchange membrane (IEM) which involves water dissociation reaction in intermediate layer. Here monopolar and bipolar IEMs with Ru (water dissociation catalyst) as intermediate layer (IL) are prepared with resin and glass fiber reinforcements using functionalized polysulfone polymer (RBPM-Ru). The prepared RBPM-Ru was characterized using universal testing machine, thermo gravimetric analysis, contact angle and chemical stability through conductivity and water absorption studies. In addition the present study highlights the new method of characterizing RBPM-Ru especially through image segmentation technique as one of the prior characteristic technique before SEM analysis to confirm its bi-layer formation in a single membrane because of its advantages like no cost requirement and less time consumption method with the same quality of accuracy. The performance of RBPM-Ru in a two-compartment electrolysytic cell was evaluated using correlated parameters such as pH, concentration and conductivity studies in both compartments. By using current voltage graph (I-V) the importance of incorporating catalytic material in IL for enhancing BPM water dissociation reaction were identified. Finally it can be concluded that RBPM-Ru was expected to have better process efficiency due to lower co-ion leakage capacity when compared with results of polystyrene-divinylbenzene (PSDVB) based BPM under similar experimental conditions.

**Keywords:** correlated parameters; image segmentation technique; lower co-ion leakage; performance comparison; RBPM-Ru; resin-fiber reinforcements; water dissociation reaction

## 1. Introduction

Membrane and membrane processes are part of our daily life. It is interdisciplinary, involving inputs from polymer chemists, physical chemists, chemical engineers and mathematicians for various purposes. Membrane technologies is one of the basic categories of water purification technologies that are used to treat water with a wide range of salinity type from brackish to sea water i.e. desalination applications (Lee *et al.* 2002, Lee and Bae 2019, Jehad *et al.* 2020). Ion exchange membranes (IEMs) constitute a very important class of membrane materials. Though resin based IEMs shows good dimensional stability than homogeneous membranes, which are the most desirable criteria for any commercially successful IEM, more ionic charges in the membrane matrix leads to low electrical resistance and high degree of swelling combined with poor mechanical stability (Vyas *et al.* 2001). Thus membranes are prepared using Ion exchange resin (IER) along with the stable, chemically resistant fabric or fiber as reinforcing material or binder that gives the necessary strength, dimensional stability and electrochemical properties to a membrane (Nagarale *et al.* 2006, Eman *et al.* 2019).

Bipolar membrane (BPMs) are type of membranes that

contain on one side an anion exchange layer (AEL) and on the other side a cation exchange layer (CEL) similar to standard anion exchange membrane (AEMs) and cation exchange membrane (CEMs) respectively. In BPM water dissociation reaction is observed to take place at the junction of the CEL and AEL called as intermediate layer (IL) (Tanaka 2007). So a high concentration of strong acid and base as fixed charges in both CEL and AEL can enhance the water dissociation reaction. In addition, presence of any type of immobilized water dissociation catalyst as IL with a smaller thickness (order of 1-10 nm) can enhance the reaction too (Strathmann *et al.* 1997).

IEM with resin can be prepared either by calendaring IER into an inert plastic film or dry moulding of inert film forming polymers and IER and then milling the mould stock or dispersing IER in a solution containing a film forming binder followed by solvent evaporation (Nagarale *et al.* 2005). BPMs were usually prepared by using commercial IEM as a precursor for ion exchange layer (IEL) (Kang *et al.* 2002, 2004, Wilhelm *et al.* 2001, Kim *et al.* 2015). It can be prepared by various methods such as loosely laminating (i.e. adhering with heat and pressure or gluing two conventional IEMs back to back with an adhesive paste) or casting a cation exchange polyelectrolyte solution (or an anion exchange polyelectrolyte solution) on a commercial AEM or prepared from the same base membrane by simultaneous functionalization at the two membrane sides (Fu *et al.* 2003) or by selective functionalization on one side to give cation

\*Corresponding author, Ph.D., Associate Professor,  
E-mail: dramanko@gmail.com

selectivity and on the other side to give anion selectivity or starting with a neutral film, BPM could be formed by introducing ionic groups on both sides of the film either by plasma treatment or by chemical treatment with specific solutions. Among all the procedures casting method was the most attractive one because of its simplicity and low cost allowing BPM with desired properties for commercial use (Hao *et al.* 2001). But in case of mix up problems due to same solvent during preparation hot press method was preferred over the casting technique. The dispersing and hot pressing lamination methods are followed in this work for monopolar and bipolar membrane preparation respectively.

Here monopolar (Reinforced cation exchange membrane - RCEM and Reinforced anion exchange membrane - RAEM) and reinforced bipolar membrane (RBPM with Ru in IL as its water dissociation catalyst) IEMs are prepared with resin and glass fiber reinforcements using polysulphone (PSu) polymer because of its excellent characteristics such as film formation, dimensional stability, thermal resistance, chemical resistance over the entire pH range, resistance in oxidative medium, high mechanical resistance etc (Subhankar *et al.* 2018). Hence the prepared BPM will possess excellent mechanical and chemical stability also. The prepared RBPM-Ru was characterized using Universal testing machine (UTM), Thermogravimetric analysis (TGA), contact angle and chemical stability through conductivity and water absorption studies for determining its mechanical strength during elongation, thermal stability, hydrophilicity nature of the IL and its durability nature after performance respectively.

An image segmentation technique is used for segmenting and dividing an image into different parts or extract dissimilar types of objects in the input images. It separates the images for identifying the objects using regions based threshold value. Also this process is simple and fast operation. When the object is hidden in background with high contrast, this method will perform effectively and reduce the cost for identifying membrane layers. It is generally used for image compression or object layer identifications (Amanpreet and Navjot 2015). The present study highlights the characterization of RBPM-Ru especially through image segmentation technique which is considered as one of the prior characteristic technique before sample was subjected to Scanning electron microscope (SEM) to confirm its bi-layer formation in a single membrane because of its advantages like no cost requirement and less time consumption method with the same quality of accuracy. The water dissociation performance results of both the prepared RBPM-Ru and commercial polystyrene-divinylbenzene-based (PSDVB) BPM in a fabricated two-compartment electrolytic cell was compared under similar experimental conditions.

## 2. Materials and methods

### 2.1 Preparation and characterization of RBPM-Ru

Resin and glass fiber reinforced monopolar (both cationic and anionic charge) and bipolar IEMs were prepared in the

'similar methodology as discussed in our earlier publication' (Venugopal and Dharmalingam 2016, Venugopal *et al.* 2017). While commercial BPM made up of PSDVB were procured from Arun Electro chemicals, Chennai. The tensile strength of the prepared RBPM-Ru is done according to ASTM D 882-91 standard using Hounsfield UTM with a cross head speed of 2 mm/min. Thermal stability and decomposition temperature of RBPM-Ru is analyzed using SDT Q 600 US analyzer (ASTM E1131), using alumina as the reference material on platinum pans and calcium sulphate as standard in a nitrogen atmosphere with the heating rate of 20°C/minute from RT to 700°C. The hydrophilic and/or hydrophobic nature of the RBPM-Ru is determined using Goniometer-sessile drop meter GBX-Digi-drop wetting and spreading studies. To investigate the morphology of the membranes, SEM micrographs are generally used. In this work, an alternative new technique so called "image segmentation" is used as one of the prior characteristic technique before SEM analysis to identify the bi-layer formation in RBPM-Ru. It has an advantage of no cost requirement and less time consumption method with the same quality of accuracy. The chemical stability of RBPM-Ru was determined using their conductivity and water absorption studies which is 'performed in the similar procedure as discussed in our publication'.

### 2.2 Gradient based layer thickness measurement using morphological operations and active contour

Image processing technique is widely used to identify the membrane layers of various thicknesses. Segmentation is a subdivision of image processing used for separating a required target region of interest from membrane image. There are different techniques used for segmentation of interest region from the images. Active contour technique is one of the active models in layer segmentation, which make use of the energy constraints and forces in the image for separating region of interest. Thus it is used in various image processing applications specifically in membrane image processing because of its advantages like no cost requirement and less time consumption method with the same quality of accuracy similar to results produced by high cost instruments. Active contour defines a separate boundary or curvature of the regions of target object for segmentation. An active contour is used for segmenting regions in different membrane through morphological gradient and is more accurate than normal gradient computing methods for color images (Hemalatha *et al.* 2018, Anh *et al.* 2012, Dhandapani *et al.* 2019, Fahimuddin *et al.* 2016, Ganesan *et al.* 2019, Sathish *et al.* 2021). Generally it is computed as in Eq. (1)

$$\nabla k = \begin{bmatrix} 1_x \\ 1_y \end{bmatrix} = \begin{bmatrix} \frac{\partial k}{\partial x} \\ \frac{\partial k}{\partial y} \end{bmatrix} \quad (1)$$

where:

$\frac{\partial k}{\partial x}$  is the derivative with respect to  $x$ , i.e., it is the gradient in  $x$  direction.

$\frac{\partial k}{\partial y}$  is the derivative with respect to  $y$ , i.e., it is the gradient in

y direction.

$\nabla k$  is the output of gradient image

The derivative of an image can be approximated by finite differences. If the central difference is used, then to calculate  $\frac{\partial u}{\partial x}$  Eq. (2) and  $\frac{\partial u}{\partial y}$  Eq. (3) are used. We can apply a 1-dimensional filter to the image  $I_m$  by convolution.

$$\frac{\partial u}{\partial x} = [-1 \ +1] * I_m \quad (2)$$

$$\frac{\partial u}{\partial y} = \begin{bmatrix} +1 \\ -1 \end{bmatrix} * I_m \quad (3)$$

where \* denotes the 1-dimensional convolution operation. Since  $2 \times 1$  filter will shift the image by half a pixel,  $3 \times 1$   $\begin{pmatrix} +1 \\ 0 \\ -1 \end{pmatrix}$  is used in order to avoid it.

The gradient direction can be calculated by the formula represented in Eq. (4),

$$\theta = \tan^{-1} \left[ \frac{l_x}{l_y} \right] \quad (4)$$

The magnitude is given in Eq. (5),

$$\sqrt{l_x^2 + l_y^2} \quad (5)$$

### 2.2.1 Algorithm for membrane layer identification

Algorithm for membrane layer identification which involves morphological operations and active contour are given below (Rad *et al.* 2017).

Input: Input image  $I_m$

Output: Identified layers  $L_1$  and  $L_2$

- Step 1: Begin
- Step 2: for each input image  $I_m$  do
- Step 3: Convert the data type of the image into double
- Step 4: Identify the Region of Interest (ROI) in membrane images
- Step 5: Create a mask
- Step 6: if (ROI)
- Step 7: Mask  $\leftarrow 1$
- Step 8: else
- Step 9: Mask  $\leftarrow 0$
- Step 10: end if
- Step 11: Convert  $I_m$  to HSV
- Step 12: Take each channel separately
- Step 13:  $N_h$  channel =  $O_h$  channel – Mask
- Step 14:  $N_s$  channel =  $O_s$  channel – Mask
- Step 15:  $N_v$  channel =  $O_v$  channel – Mask
- Step 16: Concatenate all the channels
- Step 17: Convert the concatenated channels to RGB to get the desired Layer
- Step 18: Take the old V channel alone for processing
- Step 19: Find the image gradient
- Step 20: Dilate the obtained image gradient using line structuring element
- Step 21: Reconstruct the dilated image using the fast hybrid grayscale reconstruction algorithm

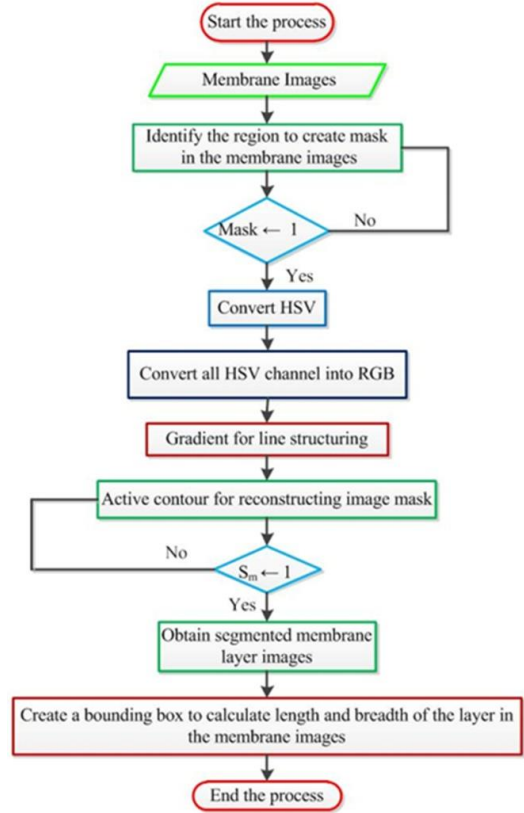


Fig. 1 Flow chart representation for layer based thickness measurement

Step 22: Apply active contour on the reconstructed image with the mask

Step 23: Obtain the segmented image  $S_m$

Step 24: On the  $S_m$  perform

Step 25: for each  $S_m$  do

Step 26: if ( $S_m == 0$ )

Step 27:  $S_m \leftarrow 1$

Step 28: else

Step 29:  $S_m \leftarrow 0$

Step 30: end if

Step 31: end for

Step 32: Extract the largest blob

Step 33: After creating a bounding box on  $L_1$ , calculate both the length and breadth of  $L_1$

Step 34: After create a bounding box on  $L_2$ , calculate both the length and breadth of  $L_2$

Step 35: end for

Step 36: End

Here  $I_m$  denotes the input image, H stands Hue, S stands for saturation and V stands for value (intensity) and  $S_m$  stands for the segmented image,  $N_h$ ,  $N_s$ ,  $N_v$  are New hue, saturation and value respectively,  $O_h$ ,  $O_s$ ,  $O_v$  are Old hue, saturation and value respectively.

### 2.2.2 Flowchart representation

Fig. 1 represents flow chart for layer based thickness measurement using morphological operations and active contour. From the input images of membrane, the region of interest is identified first to create mask in it, suppose if mask 1 is there already then convert into HSV otherwise

identify the region of interest again. After converting HSV images to RGB, image gradient is used for line structure and active contour is used for reconstructing image masks. Then obtained images are segmented and bounding box is created for calculating length and breadth of the layer in the membrane.

### 2.3 Construction and working of BPM cell

The water dissociation capabilities of both the synthesized (RBPM-Ru) and the commercial based BPM were evaluated using fabricated two compartment electro dialytic cells which are procured from Arun Electro chemicals, Chennai (Venugopal and Dharmalingam 2016, Venugopal *et al.* 2017). Total volume of each compartment is 160 cm<sup>3</sup> and an effective membrane area of BPM is 120 cm<sup>2</sup>. Initially the compartment is filled with distilled water and the membrane is placed in between the electrodes in such a way that AEL side faces towards the anode while CEL side faces the cathode. The experiment was carried out for maximum of 5h to determine the changes in pH, conductivity and concentration measurements in both the acid and base compartments (AC & BC).

## 3. Results and discussion

### 3.1 Universal testing machine (UTM)

RBPM-Ru having thickness of about 0.1 mm and width of about 20mm, withstood the applied force that tend to pull it apart for longer time and later slipped out from the tightening knobs without any damage before fracture due to the following reasons such as resin fiber reinforcement of both the monopolar membranes along with hydrophilic Ru intermediate, rigid ring structure in the polymer main chain and the intermolecular hydrogen bonds between the polar groups ( $-\text{SO}_3^-$  and  $-\text{NH}_2$ ) present in the polymer. The tensile strength and percentage elongation were found to be 140.3 MPa and 26 % respectively.

### 3.2 Thermo gravimetric analysis (TGA)

The TGA curve of RBPM-Ru from Fig.2 shows four stages of degradation from the polymer matrix. The first weight loss observed up to 120°C is due to the removal of solvent in trace amounts along with both physically and chemically bonded water molecules. Degradation of functional groups (both sulfonic and quaternary ammonium) occurs around 368°C. Loosely bound IER particles along with an intermediate molecule are lost at temperature between 385°C and 470°C. The fourth weight loss observed beyond 558°C represents the degradation of reinforced fiber along with polymer main chain.

### 3.3 Contact angle

Small contact angle measurement represents hydrophilic membrane surface as per Dias and de Pinho (1999). But the contact angle for the reinforced membranes could not be measured because of the complete absorption of water

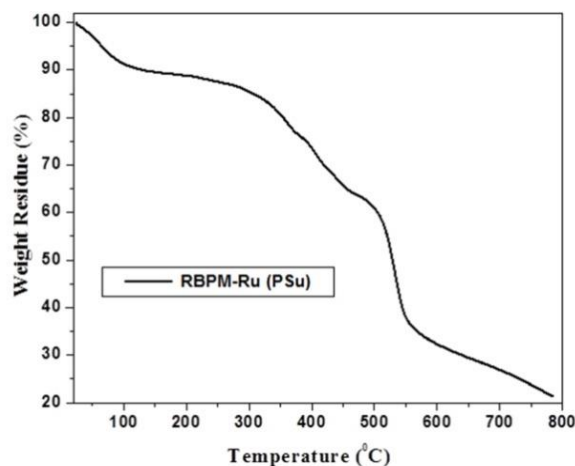


Fig. 2 TGA curve of RBPM-Ru membrane



Fig. 3 Input image for layers identification in the membrane

which reveals the increased hydrophilicity of the membranes (Sachdeva *et al.* 2008, Dai *et al.* 2001, Guan *et al.* 2005). So in case of RBPM-Ru in order to determine the nature of the IL, one face of the reinforced membrane (either CEL or AEL) was coated with IL solution and its contact angle was measured to be 59.58° which was observed to be better when compared with other catalyst mentioned in the literature survey (53.99° for RBPM-PVA coated, 50.25° for RBPM-PVP coated, 54.88° for RBPM-Pt coated). Hence RBPM-Ru can be considered to act as a good water dissociation catalyst and can increase the efficiency of the membrane performance.

### 3.4 Image segmentation technique

Fig. 3 shows the input image which is used for the image segmentation process. The input RGB image HSV as converted into HSV model of the three channels of h-hue, S-saturation and V-value before applying histogram equalization to saturation channel only to keep the image brightness. Figs. 4(a), 4(b) and 4(c) calculates the histogram for the intensity and displays a plot of the histogram. The number of bins in the histogram is determined by the image type.

Fig. 5 in general represents the sequence of process involved in the membrane layer identification such as extracted region of interest after applying the mask as represented in Fig. 5(a); Fig. 5(b) represents the canny edge detected original image; Fig. 5(c) shows the segmented image using active contour; Fig. 5(d) shows the converted image i.e., region of interest after applying active contour; Fig. 5(e) shows active contour based canny edge detected method; Fig. 5(f) shows the morphologically dilated gradient magnitude; Fig. 5(g) shows the reconstructed image after dilation; Fig. 5(h) shows the active contour output of the dilated image; Fig. 5(i) shows the extracted largest blob.

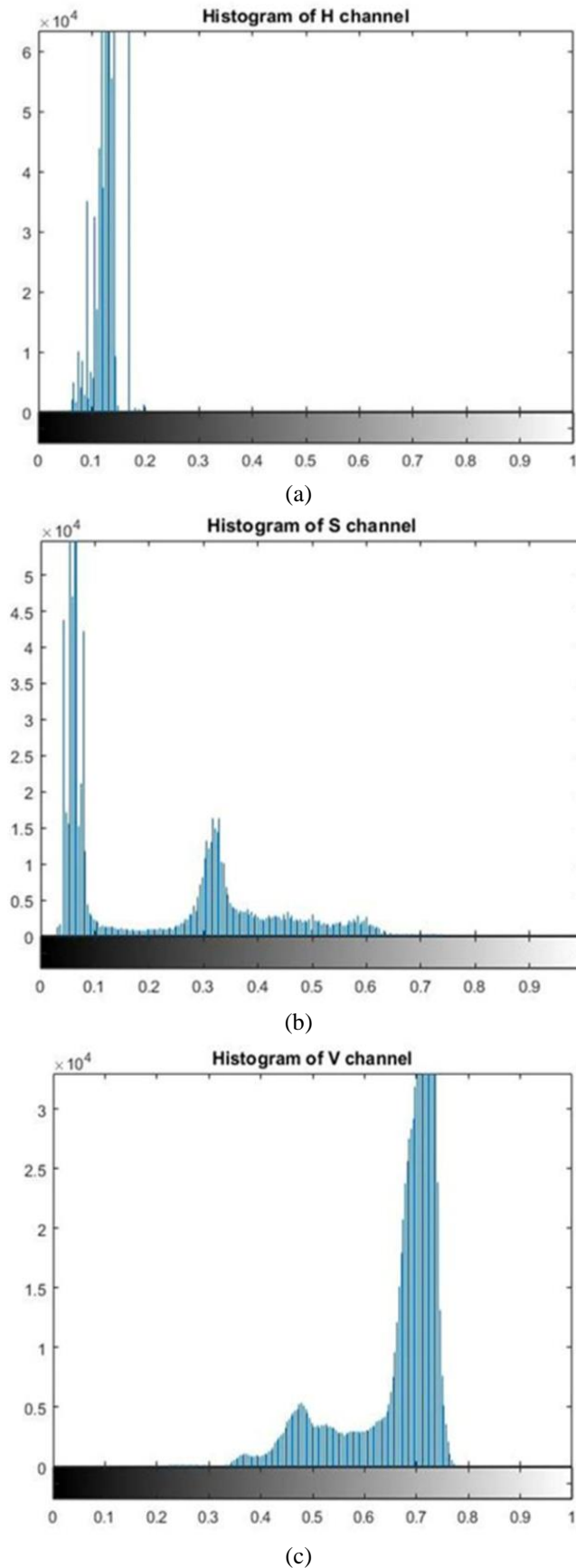


Fig. 4(a) Intensity representation of H channel; (b) Intensity representation of S channel; Intensity representation of V channel

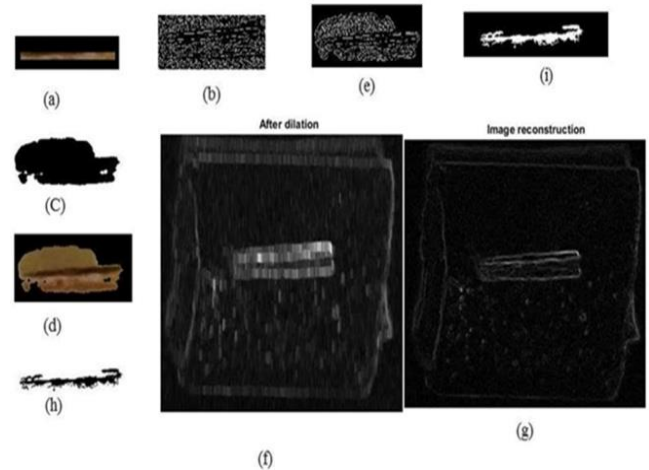


Fig. 5 Sequence of process involved in the membrane layer identification

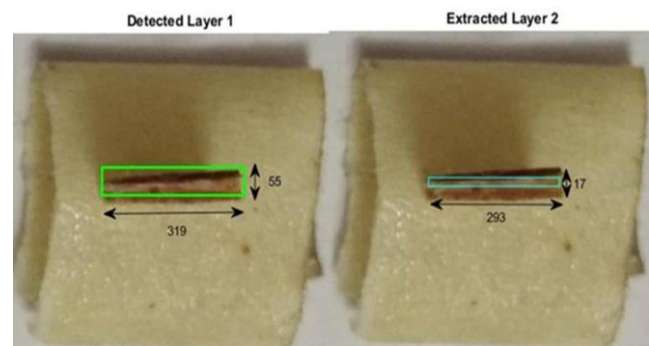


Fig. 6 Identification of layer 1 and layer 2 with respective height and width

Fig. 6 shows the identified layer 1 and layer 2 with respective height and width. The length of layer 1 and layer 2 is about 319 mm and 293 mm respectively. The width of layer 1 and layer 2 is about 55 mm and 17 mm respectively. These represents two different layer in a single membrane from the final detection.

### 3.5 Laboratory characterization

The life cycle of RBPM-Ru membrane can be determined by using Fenton's reagent which generates peroxide. Due to peroxide fast degradation mechanism hydrophilic functional groups and incorporated resins particles present on the surface are leached out from the membrane due to loosening of the fiber materials on swelling while using Fenton's reagent (Cho *et al.* 2008, Bae *et al.* 2008). However fiber reinforcement and hot pressing at higher temperature during the membrane preparation helps to control the excess water absorption by a membrane. The initial water absorption value observed for RBPM-Ru membrane is 26 % and the final value obtained after durability test is 23 %. The initial conductivity value for RBPM-Ru membrane is  $6.8 \times 10^{-3} \text{ S cm}^{-1}$  due to the presence of hydrophilic IL along with functional groups while the final conductivity value obtained after durability test is  $6.3 \times 10^{-3} \text{ S cm}^{-1}$ . From this it was observed to have lower

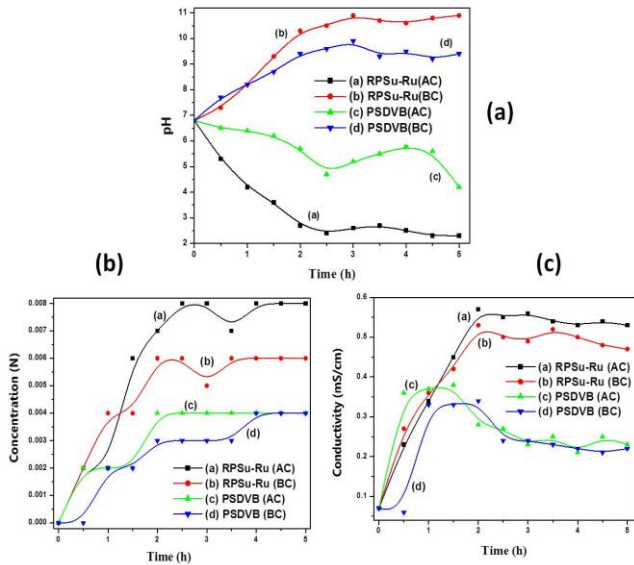


Fig. 7 Comparison of pH variation (a), Concentration changes (b) and Conductivity changes (c) with time in both AC and BC

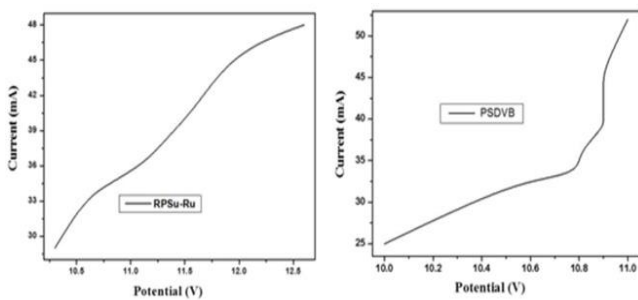


Fig. 8 Current-voltage curves for RBPM-Ru (a) and PSDVB based BPM (b)

magnitude from its initial water absorption and conductivity value.

### 3.6 Comparison of BPM performance using correlated parameters

Since BPM consists of monopolar layers which are joined together using catalytic Ru as IL, when it was placed in between the electrodes an excess  $\text{OH}^-$  and  $\text{H}^+$  ions were produced due to large electric field appearing at the membrane interface by the enhanced chemical reaction. This then migrated through the ion exchange layers into the distilled water-filled compartments resulting in the formation of acid and base. Confirmation of RBPM-Ru possessing BPM characteristics is done by analyzing the acid and base compartments using change in correlated parameters such as pH, concentration and conductivity measurements. Initially before taking readings the pH meter and conductivity meter was optimized using distilled water. From Fig. 7(a) it is obvious that with increase in time, pH of the solutions in the two compartments changed from its initial distilled water value. The solution in compartment closer to the anode side was found to be basic in nature and

the one closer to the cathode side was acidic in nature. The increasing trend in pH change with time confirmed that some ions were newly introduced only during the performance and these ions were probably protons and hydroxyl ions that were formed on either side of the BPM by means of water splitting into its ions under electrical driving force in between the electrodes. Because there was no possibility of any other ions being present by chance since only distilled water was taken in both AC and BC.

On comparing RBPM-Ru with commercial PSDVB based BPM performance in Figs. 7(a)-7(c), it is found that RBPM-Ru produce higher acidic and basic pH value, higher acid and base concentrations and conductivity values respectively during performance than PSDVB based BPM. RBPM-Ru through a steady increase in concentration showed the highest acid concentration of about 0.008N and base concentration of about 0.006N than PSDVB based BPM which showed highest acid and base concentration of about 0.004N respectively. Also it is observed that the increase in concentration was not regular during the performance for PSDVB based BPM due to the higher leakage of ions. In case of conductivity, the value increased from its initial 0.07 mS/cm to 0.56 mS/cm and 0.51 mS/cm as its maximum in AC and BC respectively and then starts to decrease from these values in both the compartments for RBPM-Ru. While the maximum was observed to be 0.38 mS/cm and 0.34 mS/cm in AC and BC respectively which then starts to decrease from these values in both AC and BC for PSDVB based BPM. The lower value or sudden decrease or leveling in both AC and BC generally represents higher leakage of ions through BPM. All these correlated parameters (pH, conductivity and concentration) represent a lesser leakage of ions that too at the later stages with respect to time through the membranes for RBPM-Ru than compared with PSDVB based BPM.

### 3.7 Current-voltage relationship in BPM

Fig. 8 (a), (b) shows the typical steady state I-V curve for the RBPM-Ru and PSDVB based BPM. If rectification would have occurred, then current could not have been found under the applied voltage in Figs. 8 (a) and (b). However, the increase in current with increasing voltage proved the occurrence of water splitting in both the BPMs (Tanioka *et al.* 1999). On comparing the potential applied during the performance for both BPMs, RBPM-Ru showed a higher value up to 12.6 V than PSDVB based BPM (11 V) for the same duration whereas the increase in current was observed to be lower for RBPM-Ru (maximum of about 48 mA) than PSDVB based BPM (maximum of about 52 mA) (Kumar and Shahi 2010). The smaller magnitude of variation in current due to ionic transportation as from Fig.8(a) when compared with Fig.8(b) represents a measure of BPM selectivity towards co-ion leakage which in turn can predict its efficiency as per Aritomi *et al.* (1996). So it could be concluded that RBPM-Ru was expected to have better process efficiency due to lower co-ion leakage capacity when compared with PSDVB based BPM. Beyond this potential, water dissociation occurs and the water splitting products ( $\text{OH}^-/\text{H}^+$ ) were also available for the

current transport which resulted in a steep increase in current.

From above discussions it is very clear that water dissociation reaction occurs in both RBPM-Ru and PSDVB based BPM which in turn supports the discussion on pH, conductivity and acid-base concentration of both BPM systems. The only reason for the difference observed in all the results between two BPMs is the presence of the Ru based IL along with fiber and resin reinforcements for RBPM-Ru whereas such modification were absent in PSDVB based BPM system. On introducing IL and resin into the membrane it became more hydrophilic by attracting water from the IEL to the space charge region. The BPM without any catalyst increases the water dissociation resistance with increase in current, because the water dissociation rate was slower than the ion transfer rate. The above obtained results thus confirm that the Ru intermediate introduced in RBPM-Ru function as a water dissociation catalyst.

#### 4. Conclusions

Monopolar (RCM and RAEM) and bipolar (RBPM with Ru in IL as its water dissociation catalyst) IEMs are prepared with resin and glass fiber reinforcements using polysulphone (PSu) polymer.

- From UTM studies, the tensile strength and percentage elongation of RBPM-Ru were found to be higher due to combination of resin fiber reinforcement of monopolar layers with Ru intermediate, rigid polymer ring structure and hydrogen bonding between functional groups.

- TGA curve of RBPM-Ru exhibited four stages of degradation while average contact angle of water on Ru coated CEL of RBPM-Ru reveal the increased hydrophilicity of the membranes.

- In addition the present study highlights the new method of characterizing RBPM-Ru especially through image processing technique instead of SEM to confirm its bi-layer formation in a single membrane because of its advantages like no cost requirement and less time consumption method with the same quality of accuracy.

- Water absorption and conductivity value shows the durable nature of RBPM-Ru.

- The water dissociation capacity nature of BPM was tested in a two-compartment electrolysytic cell. Confirmation of RBPM-Ru possessing BPM characteristics is done by analyzing the acid and base compartments using change in correlated parameters like pH, concentration and conductivity measurements.

- From I-V graph, the increase in current with increasing voltage proved the occurrence of water splitting in BPM because of incorporating catalytic material in IL.

- Finally it can be concluded that RBPM-Ru was expected to have better process efficiency due to lower co-ion leakage capacity when compared with results of PSDVB based BPM under similar experimental conditions.

#### Acknowledgement

Authors would like to thank the management of S R University, Warangal, TS for providing the facility.

#### References

- Anh, N.T.L., Kim, Y.C. and Lee, G.S. (2012), "Morphological gradient applied to new active contour model for color image segmentation", *Proceedings of the 6th International Conference on Ubiquitous Information Management and Communication*, Kuala Lumpur, Malaysia, February.
- Amanpreet K. and Navjot K. (2015), "Image Segmentation Techniques", *Int. Res. J. Eng. Technol.*, **2**(2), 944-947.
- Aritomi, T., van der Boomgaard, T. and Strathmann, H. (1996), "Current voltage curve of a bipolar membrane at high current density", *Desalination*, **104**, 13-18.
- Bae, B., Miyatake, K. and Watanabe, M. (2008), "Sulfonated poly (arylene ether sulfone) ionomers containing fluorenyl groups for fuel cell applications", *J. Membr. Sci.*, **310**, 110-118.
- Cho, C.G., Kim, S.H., Park, Y.C., Kim, H. and Park, J.W. (2008), "Fuel cell membranes based on blends of PPO with poly (styrene-b-vinylbenzylphosphonic acid) copolymers", *J. Membr. Sci.*, **308**, 96-106.  
<https://doi.org/10.1016/j.memsci.2007.09.052>.
- Dai, Y., Jian, X., Liu, X. and Guiver, M.D. (2001), "Synthesis and characterization of sulfonated poly (phthalazinone ether sulfone ketone) for ultrafiltration and nanofiltration membranes", *J. Appl. Polym. Sci.*, **79**, 1685. [https://doi.org/10.1002/1097-4628\(20010228\)79:9<1685::AID-APP180>3.0.CO;2-L](https://doi.org/10.1002/1097-4628(20010228)79:9<1685::AID-APP180>3.0.CO;2-L).
- Dhandapani, K., Venugopal, K. and Kumar, J.V. (2019), "Ecofriendly and green synthesis of carbon nanoparticles from rice bran: characterization and identification using image processing technique", *Int. J. Plast. Technol.*, **23**(1), 56-66.  
<https://doi.org/10.1007/s12588-019-09240-9>.
- Dias, C.R., de Pinho, M.N. (1999), "Water structure and selective permeation of cellulose based membranes", *J. Mol. Liq.*, **80**(2-3), 117-132.  
[https://doi.org/10.1016/S0167-7322\(99\)80003-8.dlrj](https://doi.org/10.1016/S0167-7322(99)80003-8.dlrj)
- Eman, S.M., Tarek, S.J., Heba, A., Youssef, H.F., Ahmed, M.S. and Eglal, R.S. (2019), "Desalting enhancement for blend polyethersulfone/polyacrylonitrile membranes using nanozeolite A", *Membr. Water Treat.*, **10**(6), 451-460.  
<https://doi.org/10.12989/mwt.2019.10.6.451>.
- Fahimuddin, S., Anil, K.S. and Syed, M.A. (2016), "Detection and analysis of diabetic myonecrosis using an improved hybrid image processing model", *Proceeding of 2nd International Conference on Advances in Electrical, Electronics, Information, Communication and Bio-Informatics, IEEE*, February.
- Fu, R.Q., Xu, T.W., Wang, G., Yang, W.H. and Pan, Z.X. (2003), "PEG - catalytic water splitting in the interface of a bipolar membrane", *J. Colloid Interf. Sci.*, **263**(2), 386-390.  
[https://doi.org/10.1016/S0021-9797\(03\)00307-2](https://doi.org/10.1016/S0021-9797(03)00307-2).
- Ganesan, P., Sathish, B.S., Joseph, L.M.I.L., Subramanian, K.M., Kalist, V. and Vasanth, K. (2019), "Retinal blood vessels and optical disc segmentation in branch retinal vein occluded fundus images using digital image processing techniques", *Res. J. Pharm. Technol.*, **12**(4), 1901-1906.  
<https://doi.org/10.5958/0974-360X.2019.00313.5>.
- Guan, R., Zou, H., Lu, D., Gong, C. and Liu, Y. (2005), "Polyether sulfone sulfonated by Chlorosulphonic acid and its membrane characteristics", *Eur. Polym. J.*, **41**(7), 1554-1560.  
<https://doi.org/10.1016/j.eurpolymj.2005.01.018>.
- Hao, J.H., Yu, L.X., Chen, C.X., Li, L. and Jiang, W.J. (2001), "Preparation of Bipolar Membranes (I)", *J. Appl. Polym. Sci.*, **80**(10), 1658-1663. <https://doi.org/10.1002/app.1260>.
- Hemalatha, R.J., Thamizhvan, T.R., Dhivya, A.J.A., Joseph, J.E., Babu, B. and Chandrasekaran, R. (2018), "Active contour based segmentation techniques for medical image analysis", *Med. Biol. Image Anal.*, **4**, 17.  
<https://doi.org/10.5772/intechopen.74576>.
- Jehad, M.S., Emad, M.A., Jamel, A.O. and Abdullah, M.N.

- (2020), "Water cost analysis of different membrane distillation process configurations for brackish water desalination", *Membr. Water Treat.*, **11**(5), 363-374.  
<https://doi.org/10.12989/mwt.2020.11.5.363>.
- Kim, J.S., Cho, E.H., Rhim, J.W., Park, C.J. and Park, S.G. (2015), "Preparation of bi-polar membranes and their application to hypochlorite production" *Membr. Water Treat.*, **6**(1), 27-42. <https://doi.org/10.12989/mwt.2015.6.1.027>.
- Kang, M.S., Tanioka, A. and Moon, S.H. (2002), "Effects of interface hydrophilicity and metallic compounds on water-splitting efficiency in bipolar membranes", *Korean J. Chem. Eng.*, **19**(1), 99-106.  
<https://doi.org/10.1007/BF02706881>.
- Kang, M.S., Choi, Y.J. and Moon, S.H. (2004), "Effects of inorganic substances on water splitting in ion-exchange membranes II: Optimal contents of inorganic substances in preparing bipolar membranes", *J. Colloid Interf. Sci.*, **273**(2), 533-539. <https://doi.org/10.1016/j.jcis.2004.01.051>.
- Kumar, M. and Shahi, V.K. (2010), "Heterogeneous-homogeneous composite bipolar membrane for the conversion of salt of homologous carboxylates into their corresponding acids and bases", *J. Membr. Sci.*, **349**(1-2), 130-137.  
<https://doi.org/10.1016/j.memsci.2009.11.041>.
- Lee, H., Sarfert, F., Strathmann, H. and Moon, S.H. (2002), "Designing of an electro dialysis desalination plant", *Desalination*, **142**(3), 267-286.  
[https://doi.org/10.1016/S0011-9164\(02\)00208-4](https://doi.org/10.1016/S0011-9164(02)00208-4).
- Lee, C. and Bae, S. (2019), "Special issue on advanced water treatment technologies", *Membr. Water Treat.*, **10**(3), 191-250.
- Nagarale, R.K., Gohil, G.S., Shahi, V.K. and Rangarajan, R. (2005), "Preparation and electrochemical characterization of sulfonated polysulfone cation-exchange membranes: Effects of the solvents on the degree of sulfonation", *J. Appl. Polym. Sci.*, **96**(6), 2344. <https://doi.org/10.1002/app.21630>.
- Nagarale, R.K., Gohil, G.S. and Shahi, V.K. (2006), "Recent developments on ion-exchange membranes and electro-membrane processes", *Adv. Colloid Interf. Sci.*, **119**, 97-130.  
<https://doi.org/10.1016/j.cis.2005.09.005>.
- Rad, A.E., Mohd Rahim, M.S. and Kolivand, H. (2017), "Morphological region-based initial contour algorithm for level set methods in image segmentation", *Multimed Tools Application*, **76**, 21852201.  
<https://doi.org/10.1007/s11042-015-3196-y>.
- Sachdeva, S., Ram, R.P., Singh, J.K. and Kumar, A. (2008), "Synthesis of anion exchange polystyrene membranes for the electrolysis of sodium chloride" *AIChE Journal*, **54**, 940-949.
- Sathish, B.S., Ganesan, P., Leo Joseph, L.M.I., Palani, K. and Murugesan, R. (2021), "A two-level approach to color space-based image segmentation using genetic algorithm and feed-forward neural network", *Adv. Intell. Sys. Comput.*, **1133**, 67-78. [https://doi.org/10.1007/978-981-15-3514-7\\_6](https://doi.org/10.1007/978-981-15-3514-7_6).
- Strathmann, H., Krol, J.J., Rapp, H.J. and Eigenberger, G. (1997), "Limiting current density and water dissociation in bipolar membranes", *J. Membr. Sci.*, **125**(1), 123-142.  
[https://doi.org/10.1016/S0376-7388\(96\)00185-8](https://doi.org/10.1016/S0376-7388(96)00185-8).
- Subhankar, B., Sanghamitra, M., Malini, B., Deepthi, M.V. and Sailaja, R.R.N. (2018), "Polysulfone/nanocomposites mixed matrix ultrafiltration membrane for the recovery of Maillard reaction products", *Membr. Water Treat.*, **9**(2), 105-113.  
<https://doi.org/10.12989/mwt.2018.9.2.105>.
- Tanaka, Y. (2007), "Water dissociation", *Membr. Sci. Technol.*, **12**, 139-185. [https://doi.org/10.1016/S0927-5193\(07\)12008-8](https://doi.org/10.1016/S0927-5193(07)12008-8).
- Tanioka, A., Shimizu, K., Hosono, T., Eto, R. and Osaki, T. (1999), "Effect of interfacial state in bipolar membrane on rectification and water splitting", *Colloids Surf A*, **159**(2-3), 395-404. [https://doi.org/10.1016/S0927-7757\(99\)00315-5](https://doi.org/10.1016/S0927-7757(99)00315-5).
- Venugopal, K. and Dharmalingam, S. (2016), "Composite ion exchange membrane based electro dialysis cell for desalination as well as acid and alkali productions", *Int. J. Trend Res. Develop.*, **3**(2), 631-640.
- Venugopal, K., Murugappan, M. and Dharmalingam, S. (2017), "Acid and base recovery from brine solution using PVP intermediate-based bipolar membrane through water splitting technology", *Appl. Water Sci.*, **7**(4), 1747-1759.  
<https://doi.org/10.1007/s13201-015-0346-3>.
- Vyas, P.V., Shah, B.G., Trivedi, G.S., Ray, P., Adhikary, S.K. and Rangarajan, R. (2001), "Characterization of heterogeneous anion-exchange membrane", *J. Membr. Sci.*, **187**(1-2), 39-46.  
[https://doi.org/10.1016/S0376-7388\(00\)00613-X](https://doi.org/10.1016/S0376-7388(00)00613-X).
- Wilhelm, F.G., Punt, I., van der Vegt, N.F.A., Wessling, M. and Strathmann, H. (2001), "Optimization strategies for the preparation of bipolar membranes with reduced salt ion leakage in acid-base electro dialysis", *J. Membr. Sci.*, **182**(1-2), 13-28.  
[https://doi.org/10.1016/S0376-7388\(00\)00519-6](https://doi.org/10.1016/S0376-7388(00)00519-6).

JK